

WAVELET TIME-FREQUENCY LOCALIZATION OF BI-STABLE FLOWS IN TUBE BANKS

Olinto, C. R.
PROMEC - UFRGS
e-mail: crolinto@yahoo.com.br

Indrusiak, M. L. S.
PROMEC - UFRGS
e-mail: sperbindrusiak@via-rs.net

Endres, L. A. M.
IPH – UFRGS
Av. Bento Gonçalves 9500
91501 - 970 - Porto Alegre - RS
Phone.: 55 51 3316 6669, Fax: 55 51 3319 6565
E-mail: endres@iph.ufrgs.br

Möller, S. V. *
PROMEC - UFRGS
Rua Sarmento Leite, 425, 90050-170
Porto Alegre, RS, BRAZIL
Phone:+55 51 33163228, Fax: 33164001
e-mail: svmoller@ufrgs.br

ABSTRACT

In this paper, the presence of nonstationary wakes in tube banks is studied by means of wavelet analysis of hot wire time series. The measurements were performed in a tube bank with square arrangement and pitch-to diameter ratio of 1.26, at steady and transient conditions. The Reynolds number at steady state flow, computed with the tube diameter and the flow velocity in the narrow gap between tubes is 8×10^4 . Air is the working fluid. Velocity measurements were performed after the third row using hot wire anemometry. Discrete and continuous wavelet transforms were applied to the time series to allow the analysis of phenomena in a time-frequency domain. Flow visualizations in a water channel in an enlarged arrangement with the same P/D were also used for the interpretation of the results. Results show that wavelet analysis is an adequate tool to analyze this class of phenomena, since the classical approach through Fourier transform performs an average over the entire time series and the information in time domain is lost. Results evidence the presence of a nonstationary phenomenon characterized by the alternation in the magnitude of the mean velocity measured behind the third row. This phenomenon can be very important in the heat transfer process by promoting the flow redistribution inside the bank. It can be very important as well in the flow induced vibration process by influencing the characteristic frequencies and the fluctuating pressure distribution on the tubes of the bank.

Keywords: tube banks, turbulent flows, wavelets, multiresolution analysis.

1. INTRODUCTION

Banks of tubes or rods are found in the nuclear and process industries, being the most common geometry used in heat exchangers. Attempts to increase heat exchange ratios in heat transfer equipments do not consider, as a priority of project criteria, structural effects caused by the turbulent fluid flow, unless failures occur (Païdoussis, 1982) By attempting to improve the heat transfer process, dynamic loads are increased and may produce vibration of the structures, leading, generally, to fatigue cracks and fretting-wear damage of the components, which are one of the failure sources affecting nuclear power plant performance (Pettigrew et al, 1997).

Pressure fluctuations result from velocity fluctuations at several points of the flow field (Wilmart, 1975). They are produced by the interaction of velocity gradients with velocity fluctuations and Reynolds stresses (Rotta, 1972). The amplitude of the pressure fluctuations may be influenced by velocity fluctuations at a distance comparable to the

wavelength of these fluctuations (Townsend, 1976). The search of form and magnitude of pressure and velocity fluctuations and the interdependence between these quantities is necessary for the comprehension of the complex phenomena in tube banks, since the resulting forces applied to the tubes by the turbulent flow will be given by the integral of the pressure field around each tube in the bank. From the fluctuating pressure field, a fluctuating excitation force will result, which may induce vibration of the tube if its natural frequency is present in the excitation force (Blevins, 1990).

The concern about heat transfer equipment integrity is, therefore, due to the close relationship between fluid flow around a solid surface and the vibrations induced by the flow in the structure by wall pressure fluctuations.

The classic approach to these studies is the Fourier analysis, which can give information about the frequencies involved and the interdependence of simultaneous phenomena (e. g. velocity and pressure fluctuations at different locations). An ergodic hypothesis of the time series is necessary in this case, being mean values independent of the sampling process. This hypothesis fails in time varying series, which means that Fourier analysis cannot deal with a signal that is changing over time and, therefore, its mean values are not constant. Furthermore, many processes of interest in fluid dynamics are not stationary. In accelerating flows, for instance, beside their mean values not being constant, additional phenomena may appear, as the flow velocity changes with time. Indrusiak et al. (2003) explored the use of wavelets in the study of accelerating and decelerating turbulent flows through tube banks, showing that this is an adequate tool for analyzing phenomena where the mean value is varying over time. They found behind the third row a behavior with random change between the mean velocity values measured behind one tube of the third row. The intermittence found is similar to bistable mode found for tubes placed side-by-side (Alam et al., 2003).

The purpose of this paper is to study the presence of nonstationary wakes in tube banks by means of wavelet analysis of hot wire time series and flow visualizations. This phenomenon was observed by Indrusiak et al. (2003).

2. MATHEMATICAL BACKGROUND

The Fourier transform of a discrete time series enables the study of the bulk spectral behavior of the random phenomenon represented by the series.

The Fourier transform of a finite function $x(t)$, given as a discrete time series, is defined as:

$$\hat{x}(f) = \frac{1}{2\pi} \sum_0^T x(t) e^{-ift} \quad (1)$$

The Fourier spectrum gives the energy distribution of the signal in the frequency domain and is evaluated over the entire time interval:

$$P_{xx}(f) = |\hat{x}(f)|^2 \quad (2)$$

In practice, in order to minimize the random error, was used the power spectral density function (PSD) which is the Fourier spectrum of the series smoothed over frequency intervals and over an ensemble of estimates (Bendat and Piersol, 1971).

While the Fourier transform uses trigonometric functions as basis, the bases of wavelet transforms are functions named wavelets. A wavelet is a finite energy function $\psi(t)$, with a zero average that generates an entire set of wavelet basis:

$$\psi_{a,b}(t) = \frac{1}{\sqrt{a}} \psi\left(\frac{t-b}{a}\right), \quad a, b \in \mathbb{R}, \quad a > 0 \quad (3)$$

where a and b are respectively scale and position parameters.

The continuous wavelet transform (CWT) of a function $x(t)$ is given by:

$$\tilde{X}(a, b) = \int_{-\infty}^{\infty} x(t) \psi_{a,b}(t) dt \quad (4)$$

The respective wavelet spectrum is defined as:

$$P_{xx}(a, b) = |\tilde{X}(a, b)|^2 \quad (5)$$

While the Fourier spectrum, Equation (2), gives the energy for each frequency over the entire time domain, in the wavelet spectrum, Equation (5), the energy is related to each time and scale (or frequency) (Daubechies, 1992). This characteristic of the wavelet transform allows the representation of the distribution of the energy of the transient signal over time and frequency domains, this representation is called spectrogram.

According to Percival and Walden (2000), the discrete wavelet transform (DWT) is a judicious sub sampling of the CWT, dealing with dyadic scales, and given by:

$$d(j, k) = \sum_t x(t) \psi_{j,k}(t) \quad (6)$$

where the scale and position parameters (j, k) are dyadic sub samples of (a, b).

The Fourier transform of a finite series gives only a finite number of coefficients, depending on the length of the time series, and therefore neglects the coefficients related to the higher frequencies. Anyway, these frequencies are already filtered at the acquisition process, to prevent aliasing. In the wavelet transform of a finite series, the length of the series also restricts the number of computable coefficients but, unlike the Fourier transform, the remaining coefficients are related to the lower frequencies, including the mean value of the signal, and cannot be disregarded. In practice, the DWT of a series with more than 2^J elements is computed for $1 \leq j \leq J$, being J a convenient arbitrary choice. The remaining part of the signal, containing the mean values for a scale J, is given by:

$$c(J, k) = \sum_t x(t) \phi_{J,k}(t) \quad (7)$$

where $\phi(t)$ is the scaling function associated to the wavelet function.

Any discrete time series with sampling frequency Fs can be represented by:

$$x(t) = \sum_k c(J, k) \phi_{J,k}(t) + \sum_{j \leq J} \sum_k d(j, k) \psi_{j,k}(t) \quad (8)$$

where the first term is the approximation of the signal at the scale J, which corresponds to the frequency interval $[0, Fs/2^{J+1}]$ and the inner summation of the second term are details of the signal at the scales j ($1 \leq j \leq J$), which corresponds to frequency intervals $[Fs/2^{j+1}, Fs/2^j]$

3. EXPERIMENTAL TECHNIQUE

3.1 Wind tunnel

The test section, shown schematically in Fig.1 is a rectangular channel, with 146 mm height and a width of 195 mm. Air was the working fluid, driven by a centrifugal blower, passed by a set of honeycombs and screens, before reaching the tube bank with about 1 % turbulence intensity. The air velocity, and thus the Reynolds number, can be controlled by a frequency inverter coupled to the blower supply used also to adjust velocity variation in accelerating and decelerating flows. The tube bank had a pitch to diameter ratio of 1.26, the tubes were 146mm long and had a diameter of 32.1 mm. The tubes were rigidly mounted on the upper walls and no significative gap flow between tubes and upper and lower wall was observed.

Before the tube bank, a Pitot tube, at a fixed position, was applied to measure the reference velocity for the experiments. The Reynolds number, calculated with the tube diameter and the entrance (reference) velocity is $Re = 17500$. Detailed results of pressure and velocity fluctuations in this geometry are presented by Endres and Möller (2001).

Velocity and velocity fluctuations were measured by means of a DANTEC *StreamLine* constant temperature hot-wire anemometer. Figure 2 shows the probe positions inside the tube bank.

Previous analysis of the behaviour of the test section, by means of METRA accelerometers, and of the measurement of the flow field without any obstacle, allowed identifying peaks in spectra, due to resonance of the test section, not related to the investigated phenomena. Data acquisition of velocity fluctuations were performed simultaneously by a Keithley DAS-58 A/D-converter board controlled by a personal computer.

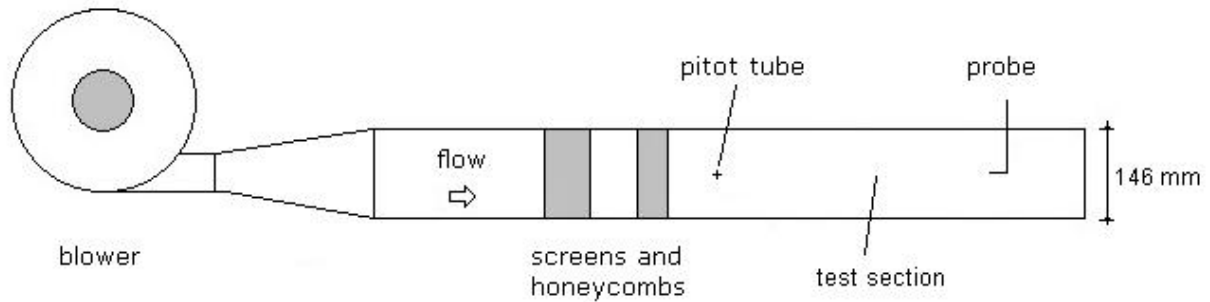


Figure 1 – Schematic view of the test section.

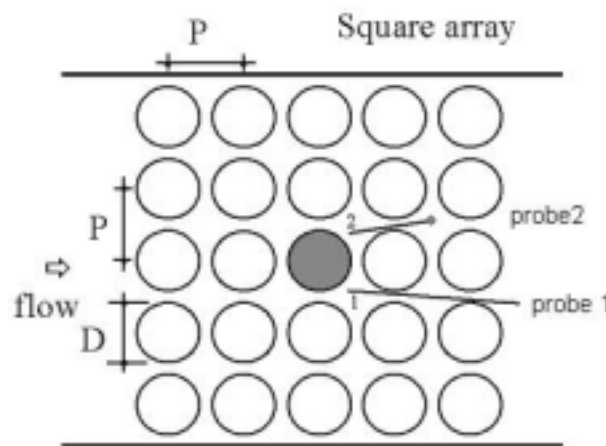


Figure 2 – Scheme of the tube bank and probe positions.

3.2 Water channel

The water tests were carried out in a closed-circuit water channel facility of the Hydraulic Research Institute IPH/ UFRGS. The tubes were fixed vertically in the test-section, where the top wall also had the function of avoiding the effect of free surface oscillations. A flood-gate and a gate valve were used to control respectively the water level and the flow rate.

Dye injection technique was used to visualize the flow structure in the arrays. The images of the flow field were recorded by a video system. Photographs presented in this paper were taken from the videos.

The test section, made of translucent plexiglas plates, is shown at Fig. 3.

The bank was made from commercial PVC tubes with diameter of 75 mm, with exception of the central one which was handmade from a translucent plexiglas plate (Fig. 4). A mirror was fixed inside this tube at the mid height of the tube, inclined 45° with the tube axis direction (Fig 4(b)). This arrangement allows the viewing of the flow inside the bank of tubes. A orifice was drilled at the wall of the tube neighbouring the plexiglas tube, in the same row (Fig. 4(a)). The dye is gravity forced through this orifice by means of an injection needle.

Flow visualizations were performed for Reynolds numbers from 5200 to 16000, computed with the tube diameter and the mean channel velocity.

Figure 5 shows the view through the mirror. In the figure the two rings out of focus are the tube wall. The circle in the center of the picture is the visualization point, where the tube wall with the dye injection orifice can be seen.

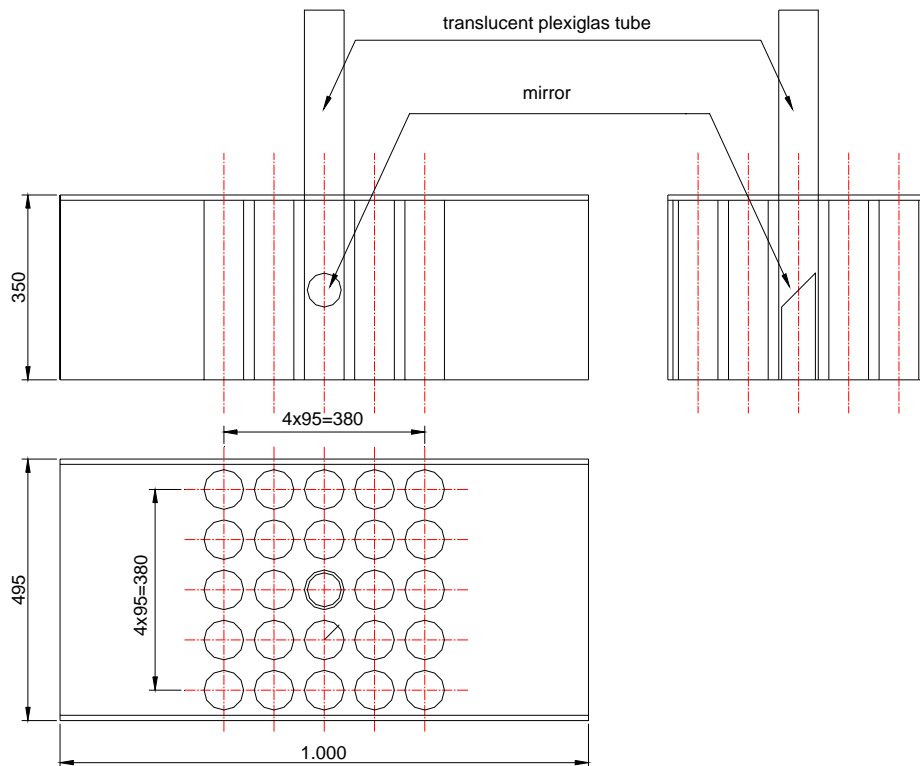


Figure 3 – Scheme of the test section for flow visualization experiments in the water channel.



Figure 4 – View of the plexiglas tube with a detail of the mirror inside the tube.



Figure 5 – Side tube observed through the mirror. Notice the dye injection orifice. Only two tubes are shown

4. RESULTS

4.1 Velocity Measurements

In order to study the phenomena occurring in the flow inside tube banks with the configuration described in Fig. 2, two velocity time series behind the central tube of the third row were obtained. The first one, with an acquisition time of 21 seconds and a frequency of 25 kHz, is a starting transient followed by a long stationary interval, is shown in Fig. 6(a). The respective wavelet approximation signals, for the frequency interval [0-12.2 Hz], Fig. 6(b), shows that the velocities of both signals switch between two mean values. This switching behavior is clearly visible at Fig. 6(b), but impossible to be identified in Fig. 6-a. Figure 7 shows the spectrograms for the first 5 seconds of the velocity signals, corresponding to the transient part. In these spectrograms the switches shown at Fig. 6-b are also present as energy fluctuations where the lower energy level of one signal is related with the higher energy levels of the other. The energy of the fluctuations is related to the mean velocity: the higher energy levels of the fluctuations correspond to lower mean velocities.

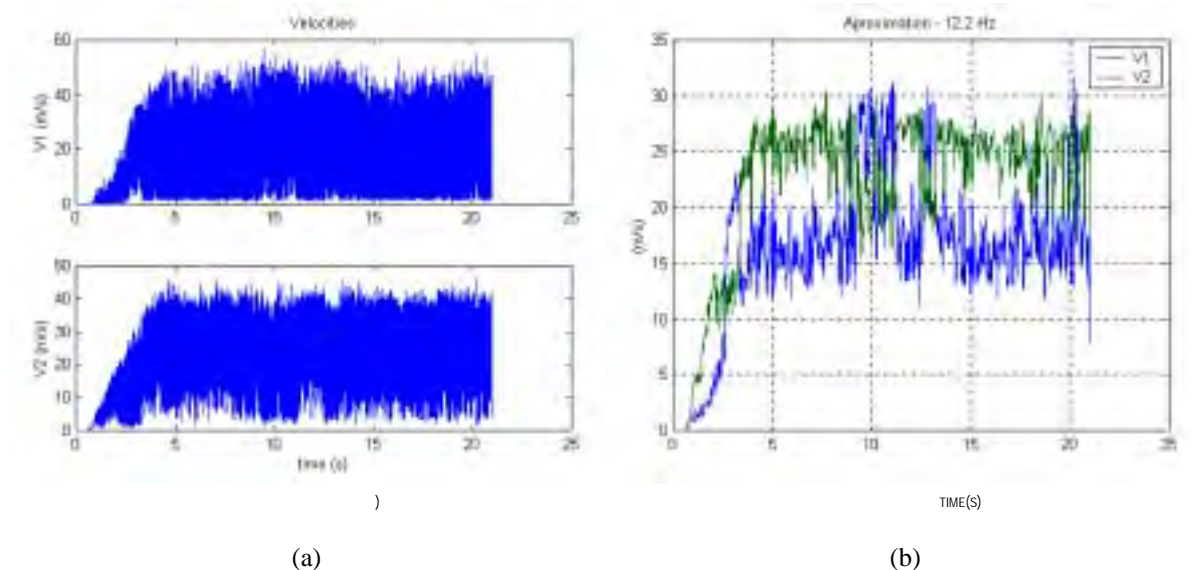


Figure 6 – Instantaneous velocities - first acquisition (a) and corresponding wavelet discrete

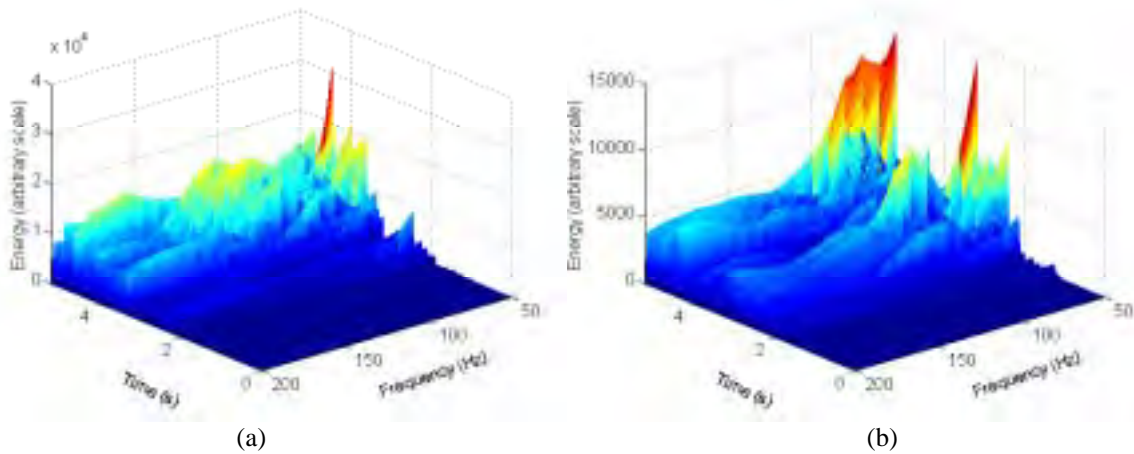


Figure 7 – Spectrograms of the velocity signals - first acquisition: (a) V1 (b) V2

Another acquisition, where a similar phenomenon is present is shown at Fig.8(a). In the wavelet approximation signals (Fig.8(b)), it is possible to identify that the mean velocity V2 changes at around 20 seconds whilst the mean velocity V1 remains unchanged.

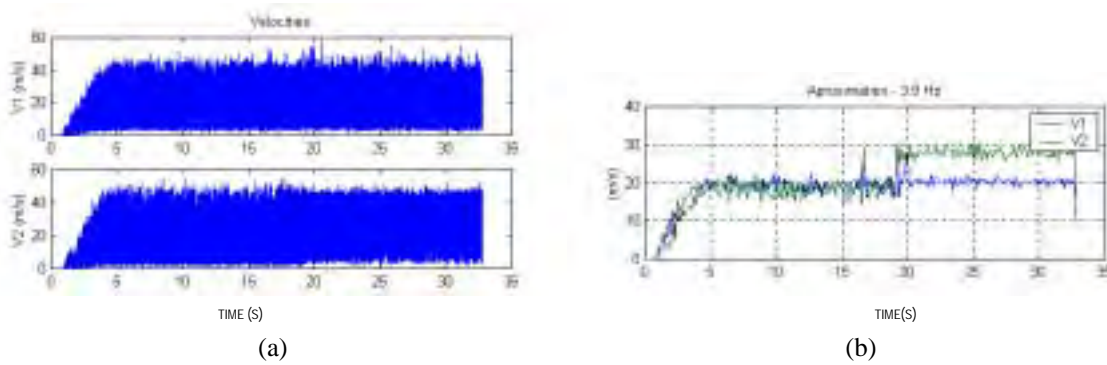


Figure 8 – Instantaneous velocities - second acquisition (a) and corresponding wavelet discrete transform (b).

Figure 9 shows spectrograms of the signals V1 and V2 for time interval 15 to 23 seconds comprising the time location where the velocities change their behavior. One can verify that, for velocity V2 (Fig. 9(b)), the increase in the velocity value is accompanied by a reduction of the energy of the fluctuation. This is not so evident at V1 spectrogram signal.

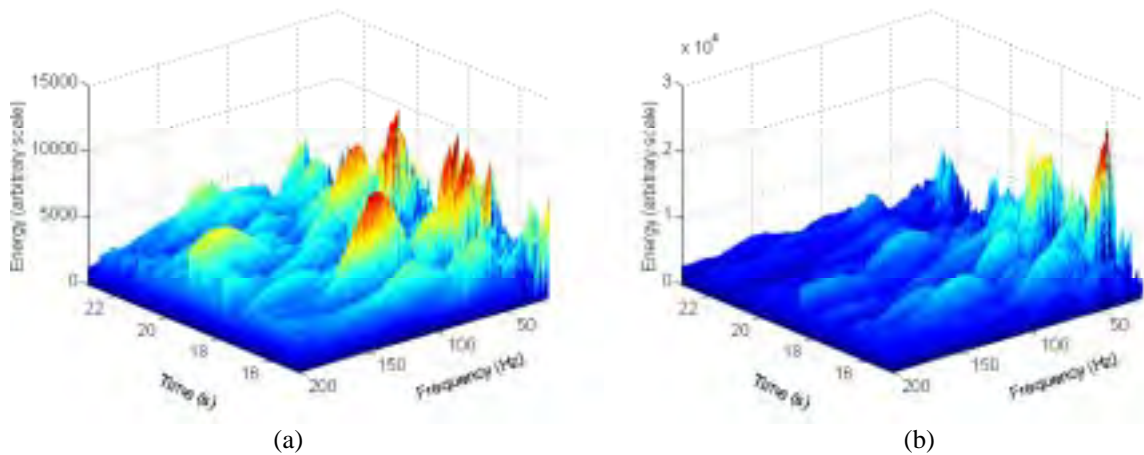


Figure 9 – Spectrograms of the velocity signals - second acquisition: (a) V1; (b) V2.

In order to characterize the two ways as the air flows inside the bank, the steady part of the signal was divided into two groups: mode A from 8 s to 16.2 s, and mode B from 22 to 30.2 s. Their statistical characteristics are shown at Tab. 1 and Fig. 10 shows the probability density functions. The reference velocity measured upstream at Pitot tube was 7.24 m/s.

Table 1 – Statistical characteristics of the velocity signal divided into two flow modes

	mode A		mode B	
	V1	V2	V1	V2
Mean velocity	19.22	18.28	20.36	28.02
Standard deviaton	8.76	9.81	8.12	8.53
Skewness	0.48	0.65	0.39	-0.43
Kurtosis	2.49	2.64	2.73	2.73

The most important change in the statistical features is the mean velocity jump at velocity V2. Another characteristic is the change in the skewness signal of velocity V2: in the mode A it is positive while in the mode B it becomes negative demonstrating the presence of different distributions of the velocity fluctuation.

No important peaks can be observed in the velocity spectra shown in Fig. 11. This is the behavior expected inside in line tube banks, especially after the third row, according to the results by Ziada et al., 1989.

Additional data acquisitions were made inside the tube bank, changing the initial conditions and introducing flow disturbances. In some cases, new flow modes were generated, in other cases, the original flow mode did not change. In all the cases investigated, a rigorous evaluation was performed to identify the presence of instabilities. The results are not yet conclusive and therefore not shown in this paper.

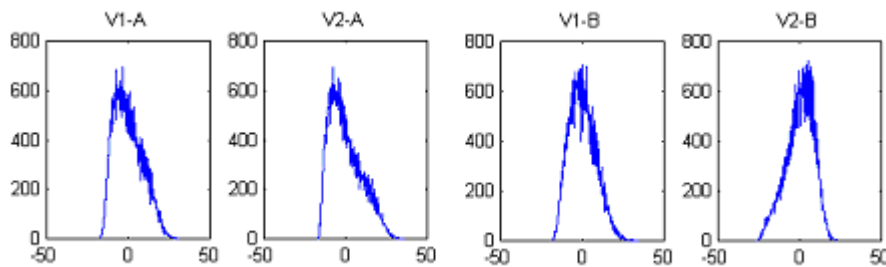


Figure 10 – Probability density functions of the velocity signals.

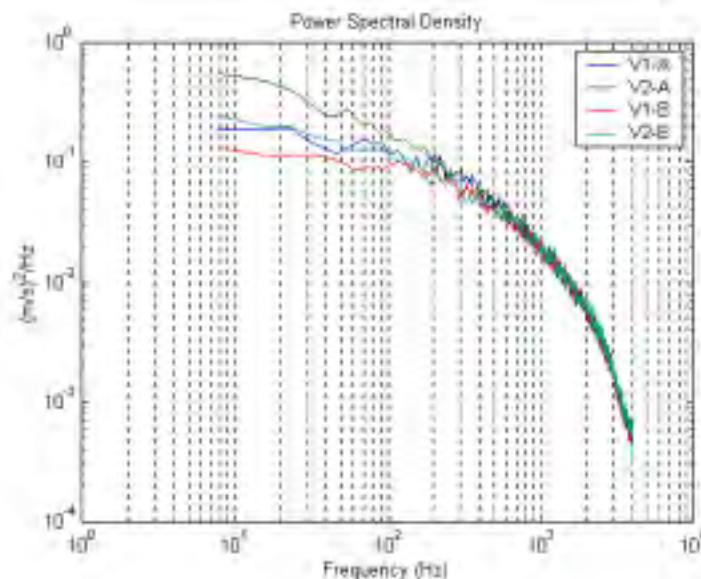


Figure 11 – Fourier spectra of velocity signals, modes a and b

4.2 FLOW VISUALIZATIONS

The flow was visualized at two points: at the entrance and at the middle of the bank, in the gap between the translucent tube and the tube with the orifice for dye injection. Figure 12 shows the behavior of the flow at the entrance. Dye was injected 270 mm upstream the bank and travels aligned with the channel axes until it reaches the bank, where it deviates strongly to one side, traveling and spreading at diagonal direction. The side of the deviation is constant for each run of the experiment but changes randomly from one run to another.

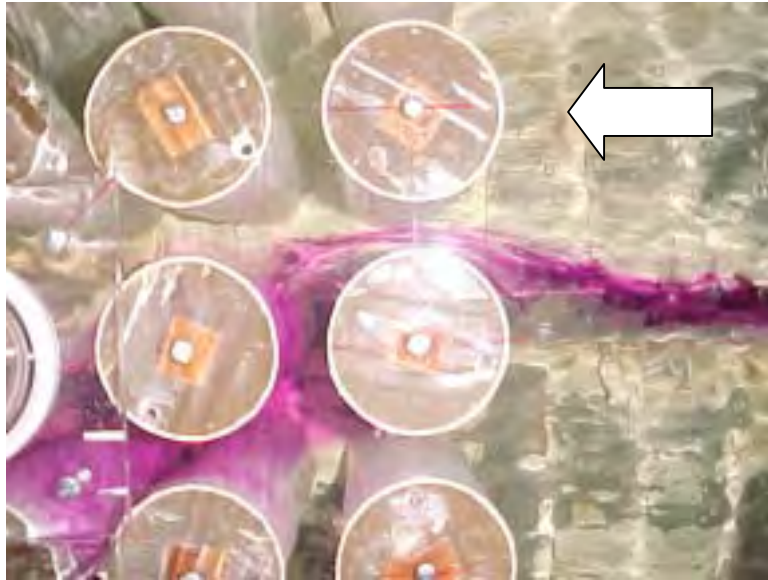


Figure 12 - Biased and spread flow at left diagonal direction (seeing from upstream to downstream)

The visualizations performed at the middle of the bank, according to the mounting scheme of Fig. 3, are shown at Fig. 13. At each run of the experiment the flow is deviated either upwards (a) or downwards (b), in correspondence with the right or left orientation at the entrance, respectively.

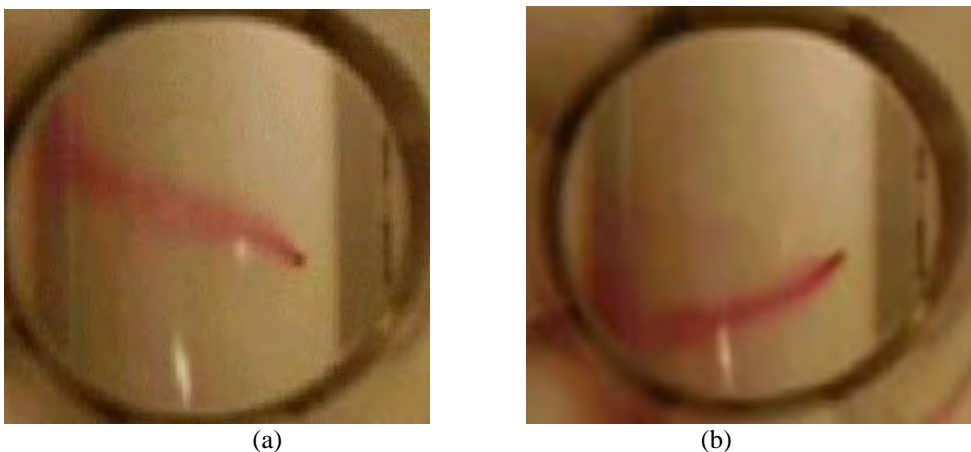


Figure 13 - Visualization of the dye flow on the tube surface through the mirror inside the plexiglass tube: (a) upward flow, (b) downward flow.

The visualizations described above evidence that the three orthogonal components of the flow through the tube bank must be taken into account to describe correctly the phenomena. These two distinct behaviors of the flow may be related to the two modes described at the previous section.

5. CONCLUSIONS

In this work, the velocity behind the third row in a tube bank with square arrangement and pitch-to-diameter ratio of 1.26 was measured. Visualization in a water channel of a flow through a tube bank with the same pitch-to-diameter ratio was also made.

A nonstationary phenomenon inside a bank of tubes with quadrangular arrangement was identified and characterized by the variation of the mean values of the velocity signals measured at fixed points. The time interval and points of switching of velocity are random distributed along the measured series, being distinct of the jet instabilities found by Ziada and Oegören (1992) at the lanes between tubes of similar configuration.

At the water channel experiments, each run had a constant behavior. Nevertheless, the flow presented two distinct behaviors, related to a strong transversal component that crosses the lanes between the tubes. It was also observed that this transversal component is associated to a vertical component that directs the flow upwards or downwards, depending on the left or right orientation of the transversal component. The observations described above show that for the flow past tube banks with square arrangements and pitch to diameter ratios of 1.26, the three orthogonal components of the flow are equally significant. The usual two-dimensional approach of this kind of phenomena may lead to mistakes and should be carefully considered in the interpretation of the results.

The three-dimensional behavior of the flow is responsible for a mass redistribution, leading to localized unexpected velocities values and Strouhal numbers, at the studied geometry. This can explain the Strouhal number distribution observed in the Fitzhugh diagrams (Blevins, 1990).

REFERENCES

- Alam, M. M., Moriya, M. and Sakamoto, H., (2003), Aerodynamic characteristics of two side-by-side circular cylinders and application of wavelet analysis on the switching phenomenon, *Journal of Fluids and Structures*, vol. 18, pp. 325–346
- Blevins, R. D., (1990), “Flow-Induced Vibration”, 2nd Ed., Van Nostrand Reinhold, New York.
- Bendat, J. S., Piersol, A. G., (1971), “Random Data: Analysis and Measurement Procedures”, Wiley-Interscience.
- Daubechies, I., (1992), “Ten Lectures on Wavelets”, Society for Industrial and Applied Mathematics, Philadelphia. Pennsylvania.
- Endres, L. A. M. and Möller, S. V. (2001). “On the Fluctuating Wall Pressure Field in Tube Banks”, *Nuclear Engineering and Design*, Vol. 201, pp. 13-26.
- Indrusiak, M. L. S., Goulart, J. N., Olinto, C. R., Möller, S. V., (2003). “Wavelet Time-Frequency Analysis of Accelerating and Decelerating Flows in a Tube Bank”, *Trans. SMiRT 17, 17th International Conference on Structural Mechanics in Reactor Technology*, paper J 275, Prague.
- Paidoussis, M. P., (1982), “A review of flow-induced vibrations in reactors and reactor components”, *Nuclear Engineering and Design*, Vol. 74, pp. 31-60.
- Percival, D. B., Walden, A. T., (2000), “Wavelet Methods for Time Series Analysis”, Cambridge University Press, Cambridge, UK.
- Pettigrew, M. J., Taylor, C. E., Fisher, N. J., Yetisir, M., Smith, B. A. W., (1997), “Flow-induced vibration: recent findings and open questions”, *Trans. SMiRT 14, 14th International Conference on Structural Mechanics in Reactor Technology*, V. 0, pp. 19-48, Lyon.
- Rotta, J. C., (1972), “Turbulente Strömungen”, B. G. Teubner: Stuttgart.
- Townsend, A. A., (1976), “The structure of turbulent shear flow”, Cambridge U. P., Cambridge, UK.
- West, G. S., Apelt, C. J., (1982), “The effects of tunnel blockage and aspect ratio on the mean flow past a circular cylinder with Reynolds numbers between 10^4 and 10^5 ”, *J. Fluid Mech.*, v. 114, pp. 361-377.
- Willmarth, W. W., (1975), “Pressure fluctuations beneath turbulent boundary layers”, *Ann. Rev. of Fluid Mech.*, Vol. 7, pp. 13-88.
- Ziada, S., Oengören, A., Bühlmann, E. T., (1989), “On Acoustical Resonance in Tube Arrays. Part I: Experiments”, *Journal of Fluids and Structures*, Vol. 3, pp. 293-314.
- Ziada, S., Oegören, A., (1992), “Vorticity Shedding and Acoustic Resonance in an in-line Tube Bundle – Part I: Vorticity Shedding”, *Journal of Fluids and Structures*, Vol. 6, pp. 271-292.